

# Backward line tracking control of a radio-controlled truck and trailer

Claudio Altafini\*

Alberto Speranzon

Optimization and Systems Theory  
Royal Institute of Technology  
Stockholm, Sweden  
altafini@math.kth.se

Signals, Sensors and Systems  
Royal Institute of Technology  
Stockholm, Sweden  
albspe@s3.kth.se

## Abstract

A control scheme is proposed for the backward line tracking problem of a truck with trailer. It combines two different regulators, one for backward motion and the other for forward, in a switching scheme that assures convergence to the desired line. The scheme has been implemented and successfully used to reverse a radio-controlled vehicle.

## 1 Introduction

This paper describes a feedback control scheme used to stabilize the backward motion of the radio-controlled truck and trailer shown in Figure 1. The vehicle re-

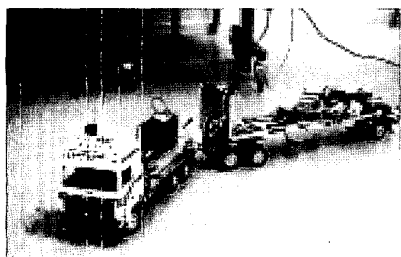


Figure 1: The radio-controlled truck and trailer

produces in detail the geometry of a full-scale lorry; it has four axles, actuated front steering and actuated second axle to govern the longitudinal motion. Like the real one it presents saturations on the steering angle and on the two relative angles between the bodies. It is equipped with potentiometers and dif-

ferential encoders so that full state feedback is possible. Our control task is to drive the system backward along a preassigned straight line, avoiding jack-knife effects on the angles. There is a moderate literature on backward steering control of multiple wheeled vehicles reporting on experimental results achieved with different control techniques and with different kinds of vehicles, mainly especially built laboratory mobile robots, see for example [4, 8, 12]. Numerous papers treat the backing problem with tools spanning from neural network [9], fuzzy control [5, 12], learning, genetic algorithms and expert systems [3, 10]. Only a few works make use of more theoretical tools stemming from the literature on control of kinematic vehicles (overviewed for example in [7]), see [6, 11]. According to such formalism, our system is a general 3-trailer, general because of the kingpin hitching between the second axle and the dolly (see [1]). From a system theory point of view, the control problem is quite challenging: it is an unstable nonlinear system with state and input constraints. The “reduced” control goal of stabilization along a line (instead of a point) allows to consider a system with controllable linearization so that local asymptotic stability can be achieved via Jacobian linearization. Still, the combination of instability and saturations makes the task impossible with a single controller. The scheme we use consists of a switching controller with a logic variable (the sign of the longitudinal velocity input  $v$ ) that allows switching between the two different modes, backward (open-loop unstable) and forward (open-loop stable), each of them governed by a linear state feedback designed via linear quadratic techniques on the Jacobian linearizations. Since  $v$  is a control input for the system, it becomes the natural choice for a logic variable that switches between two regimes governed by two different feedback controllers. In order to automatically select the logical value of  $v$ , a suitable partition of the state space has to be given. The crossing of

\*This work was supported by the Swedish Foundation for Strategic Research through the Center for Autonomous Systems at KTH

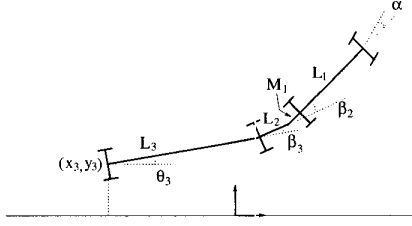


Figure 2: The kinematic model of the truck and trailer of Fig. 1

the switching surfaces of the partition and the direction of crossing provide the feedback information to  $v$ . In synthesis, the switching can be seen as an extra feedback loop around the two different closed loop modes. The switching surfaces and the switching logic are designed in such a way that the desired equilibrium inside the backward motion regime is given the character of global attractor from all the initial conditions in a prespecified domain.

## 2 Kinematic equations and linearization

The differential equations describing the kinematic of the vehicle under exam (see Figure 2 for notation) can be found for example in [1]:

$$\begin{aligned} \dot{x}_3 &= v \cos \beta_3 \cos \beta_2 \left( 1 + \frac{M_1}{L_1} \tan \beta_2 \tan \alpha \right) \cos \theta_3 \\ \dot{y}_3 &= v \cos \beta_3 \cos \beta_2 \left( 1 + \frac{M_1}{L_1} \tan \beta_2 \tan \alpha \right) \sin \theta_3 \\ \dot{\theta}_3 &= v \frac{\sin \beta_3 \cos \beta_2}{L_3} \left( 1 + \frac{M_1}{L_1} \tan \beta_2 \tan \alpha \right) \end{aligned} \quad (1)$$

$$\begin{aligned} \dot{\beta}_3 &= v \cos \beta_2 \left( \frac{1}{L_2} \left( \tan \beta_2 - \frac{M_1}{L_1} \tan \alpha \right) - \right. \\ &\quad \left. - \frac{\sin \beta_3}{L_3} \left( 1 + \frac{M_1}{L_1} \tan \beta_2 \tan \alpha \right) \right) \end{aligned} \quad (2)$$

$$\dot{\beta}_2 = v \left( \frac{\tan \alpha}{L_1} - \frac{\sin \beta_2}{L_2} + \frac{M_1}{L_1 L_2} \cos \beta_2 \tan \alpha \right) \quad (3)$$

The two inputs of the system are the steering angle  $\alpha$  and the longitudinal velocity at the second axle  $v$ . Call  $\mathbf{p} = [y_3 \theta_3 \beta_3 \beta_2]^T$  the configuration state obtained neglecting the longitudinal component  $x_3$ .

In a compact way, the state equations are written as:

$$\dot{\mathbf{p}} = v(\mathcal{A}(\mathbf{p}) + \mathcal{B}(\mathbf{p}, \alpha)) \quad (4)$$

The sign of  $v$  decides the direction of motion.  $v < 0$  corresponds to backward motion. The entire state is measured via two potentiometers on the relative angles  $\beta_2$  and  $\beta_3$  and a pair of encoders on the two wheels of the rearmost axle. No inertial measure is available.

**State and input saturations** Both the relative angles  $\beta_2$  and  $\beta_3$  present hard constraints:

$$|\beta_2| \leq \beta_{2s} = 0.6 \text{ rad} \quad (5)$$

$$|\beta_3| \leq \beta_{3s} = 1.3 \text{ rad} \quad (6)$$

These limitations are due to the front and rear body touching each other and to the dolly touching the wheels. They are particularly critical since for back-up maneuvers the equilibrium point is unstable and jack-knife effects appear on both angles. Also the input has a saturation:

$$|\alpha| \leq \alpha_s = 0.43 \text{ rad} \quad (7)$$

The steering servosystem tolerates very quick variations, so we do not assume any slew rate limitation in the steering signal.

**Jacobian linearization along straight lines** The system (4) is homogeneous in the longitudinal input  $v$ . Fixing  $v$  as a given nonnull function means having a drift component which gives a nonvanishing term to the differential equations of the system. The steering angle  $\alpha$  can be used to give asymptotic stability to the system along a trajectory. The equilibrium point of  $\mathbf{p}$  is the origin  $\mathbf{p}_e = 0$  and it corresponds to a nominal value of the steering input  $\alpha_e = 0$ . The linearized system is

$$\dot{\mathbf{p}} = v(\mathbf{A}\mathbf{p} + \mathbf{B}\alpha) \quad (8)$$

where

$$\mathbf{A} = \begin{bmatrix} 0 & 1 & 0 & 0 \\ 0 & 0 & \frac{1}{L_3} & 0 \\ 0 & 0 & -\frac{1}{L_3} & \frac{1}{L_2} \\ 0 & 0 & 0 & -\frac{1}{L_2} \end{bmatrix} \quad \mathbf{B} = \begin{bmatrix} 0 \\ 0 \\ -\frac{M_1}{L_1 L_2} \\ \frac{L_2 + M_1}{L_1 L_2} \end{bmatrix} \quad (9)$$

## 3 Controllers for backward and forward motion

### 3.1 Backward controller

Consider the straight line backing case. The linearization (8) is open-loop unstable: the characteristic poly-

nomial of the uncontrolled system is

$$\det(sI - vA) = s^2 \left( s + \frac{v}{L_2} \right) \left( s + \frac{v}{L_3} \right) \quad (10)$$

Since (8) is controllable, the origin of the nonlinear system (4) locally can be made an asymptotically stable equilibrium by linear state feedback. We treat it as a linear quadratic optimization problem and in the weight assignment we use the rule of thumb of trying to have decreasing closed-loop bandwidths when moving from the inner loop to the outer one in a nested loopshaping design. In fact, the relative displacement  $y_3$  comes after a cascade of two integrators from the relative angles as can be seen on the linearization (9). It turns out that such a heuristic reasoning is very important in the practical implementation in order to deal with the saturations.

It is in general difficult to draw conclusion on the invariance properties of the flow of a nonlinear system. If in addition one takes into account the state and input constraints (5)-(7), then an analytic description becomes almost impossible. Therefore, in order to obtain estimates of the region of attraction of the linear controller

$$\alpha = -K_B \mathbf{p} \quad K_B = [k_{B_1} \dots k_{B_4}] \quad (11)$$

and of the contractivity of the resulting integral curves, we rely on the numerical simulation of the closed-loop behavior of the original nonlinear system (4) paired with the linear controller (11)

$$\dot{\mathbf{p}} = \mathcal{F}_B(\mathbf{p}) = v(\mathcal{A}(\mathbf{p}) + \mathcal{B}(\mathbf{p}, -K_B \mathbf{p})) \quad (12)$$

In order to obtain a graphical representation of the results, in the following we neglect the  $y_3$  component of the state space which is by far the less critical one with the LQ controller under use.

The cloud of initial conditions that represents the region of attraction closely resembles an ellipsoid in  $\hat{\mathbf{p}} = [\theta_3 \ \beta_3 \ \beta_2]^T$  space. The fitting of an ellipsoid  $\hat{\mathcal{E}}$  strictly contained in the set of successful initial conditions can be done by direct investigation, see Figure 3. The principal axes  $\hat{\mathbf{q}} = [q_1 \ q_2 \ q_3]^T$  of the ellipsoid are related to  $\hat{\mathbf{p}}$  by an orthogonal transformation:

$$\hat{\mathbf{p}} = \hat{R}_{\mathcal{E}} \hat{\mathbf{q}} \quad \hat{R}_{\mathcal{E}} \in SO(3)$$

Calling  $\varepsilon_1$ ,  $\varepsilon_2$  and  $\varepsilon_3$  the semiaxes of  $\hat{\mathcal{E}}$ , the ellipsoid is given by the algebraic equation

$$\hat{\mathcal{E}} = \left\{ \frac{q_1^2}{\varepsilon_1^2} + \frac{q_2^2}{\varepsilon_2^2} + \frac{q_3^2}{\varepsilon_3^2} = 1 \right\} \quad (13)$$

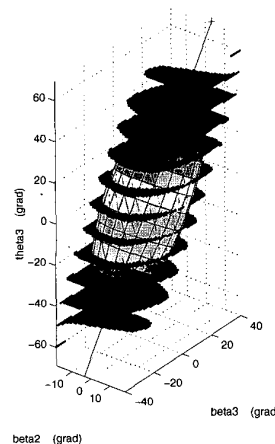


Figure 3: The successful initial conditions and the fitted ellipsoid  $\hat{\mathcal{E}}$ .

Taking into account also the  $y_3$  component of the initial conditions, the ellipsoid  $\mathcal{E} \in \mathbb{R}^4$  is given by

$$\mathcal{E} = \left\{ \frac{q_1^2}{\varepsilon_1^2} + \frac{q_2^2}{\varepsilon_2^2} + \frac{q_3^2}{\varepsilon_3^2} + \frac{q_4^2}{\varepsilon_4^2} = 1 \right\} \quad (14)$$

with  $\varepsilon_4 \gg \varepsilon_i$ ,  $i = 1, 2, 3$ . In  $D$  the difference with respect to Figure 3 can hardly be appreciated.

From Figure 3, we draw the qualitative conclusion that for the closed-loop nonlinear system  $\hat{\mathcal{E}}$  is a positively invariant set.

### 3.2 Stabilization for forward motion

When  $v > 0$ , in (10) the two unstable poles move on the open left half of the complex plane. Considering the subsystem  $\hat{\mathbf{p}}$  means neglecting one of the two poles in the origin. The origin of  $\hat{\mathbf{p}}$  is asymptotically stabilizable by linear feedback and this time convergence for the nonlinear system is a less critical problem. The reason for neglecting  $y_3$  when moving forward is again the same: the closed loop mode relative to  $y_3$  has a natural time constant higher of several orders of magnitude when compared to the other states.

Assume for example  $v = 1$ . Extracting from (9) the three dimensional system  $(\hat{A}, \hat{B})$ , linearization around the origin of (1)-(3), it is possible to choose a linear feedback

$$\alpha = \hat{K}_F \hat{\mathbf{p}} \quad (15)$$

such that the closed loop system  $\dot{\hat{\mathbf{p}}} = v(\hat{A} - \hat{B}\hat{K}_F)\hat{\mathbf{p}}$  is asymptotically stable and has three distinct real

modes. The practical rule here for the selection of the eigenvalues is to try to have all 3 closed-loop poles of the same order of magnitude. The unavoidable input saturation will not destroy stability anyway.

A forward feedback on  $y_3$  is of no practical interest because of the long time constant of the  $y_3$  mode.

## 4 Switching controller

The region of attraction of the backward controller is only a subset  $\hat{\mathcal{E}}$  of the entire domain  $D$ . Starting from outside  $\hat{\mathcal{E}}$ , it is necessary to first drive forward for example with a controller like (15) until the system enters inside  $\hat{\mathcal{E}}$  and only then switch to backward motion. When reversing, the main manifestation of a destabilizing perturbation is a jack-knife effect on the relative angles. Just like on a full-scale truck and trailer vehicle, the only way to recover from such a situation is to move forward and try again. So, in order to guarantee stability of the backward motion in  $D$  and not only inside the ellipsoid  $\hat{\mathcal{E}}$  for the nominal model and in order to cope with the perturbations, one single controller is not enough. The switching variable between the two controllers is the longitudinal velocity  $v$ . For example we assume that  $v \in \{-1, +1\} \triangleq \mathcal{I}$ . The backward regime is selected by  $v = -1$  and the forward one by  $v = +1$ . Since the longitudinal input  $v$  is a control input, if we assume that  $v \in \mathcal{I}$  then  $v$  becomes a controlled logic variable. Moreover, if the selection of the logic value of  $v$  is made according to a partition of the state space, the overall system with multiple controllers becomes a feedback controlled system. This is feasible in our case since we have on-line full state information available.

### 4.1 Selection of the two switching surfaces

Two are the switching surfaces that delimit the partition of the state space, and their crossing in a prescribed direction by the flow of the system induces a sign change in  $v$ . This in its turn causes the inversion of the direction of motion and induces the activation of the corresponding linear state feedback controller. These switching surfaces, call them  $\mathcal{S}_{-+}$  and  $\mathcal{S}_{+-}$  have to be chosen such that they give to the point  $\mathbf{p} = 0$  of the backward motion the character of global attractor (in  $D$ ).

Since in both regimes the origin is the closed-loop local asymptotically stable equilibrium point, we choose

both  $\mathcal{S}_{-+}$  and  $\mathcal{S}_{+-}$  as closed hypersurfaces in  $\mathbb{R}^4$  containing the origin in their interior.

**The switching surface from forward to backward motion:  $\mathcal{S}_{+-}$**  From Section 3.1,  $\mathcal{S}_{+-}$  has to be contained inside  $\mathcal{E}$ . The simplest choice is to consider  $\mathcal{S}_{+-} = \mathcal{E}_\rho$  for some  $\rho$  such that  $\frac{1}{2} < \rho < 1$ . The trade-off is the following:

- if  $\mathcal{S}_{+-}$  is large ( $\rho \rightarrow 1$ ) the system will be sensitive to disturbances and more easily destabilized by perturbations (meaning more switches can occur);
- if  $\mathcal{S}_{+-}$  is small ( $\rho \rightarrow \frac{1}{2}$ ) the forward regime will be very long, which is often unacceptable for practical implementations.

Ellipsoids smaller than  $\mathcal{E}_{\frac{1}{2}}$  are also not recommendable for other reasons, like the possibility of being completely “jumped over” in case of relevant sensor error.

**The switching surface from backward to forward motion:  $\mathcal{S}_{-+}$**  Such a switching surface has to “tell” the system that backing is not going well and the trailers need to be realigned. The choice is quite flexible, the only constraint is that  $\mathcal{S}_{+-}$ ,  $\mathcal{S}_{-+}$  and the sides of  $D$  must not intersect. In particular the set distance between  $\mathcal{S}_{+-}$  and  $\mathcal{S}_{-+}$  gives the hysteresis between the two regimes. If this distance is positive, problems like chattering will be avoided. One simple choice for  $\mathcal{S}_{-+}$  is for example to use a cube in  $\mathbb{R}^4$  which is a rescaling of  $D$  by a factor less than 1.

**Control logic for  $v$**   $D$  is divided into three nonintersecting regions:

- $\mathcal{C}_-$  = region inside  $\mathcal{S}_{+-}$  where  $v = -1$ ;
- $\mathcal{C}$  = region between  $\mathcal{S}_{-+}$  and  $\mathcal{S}_{+-}$  where  $v$  can be either  $+1$  or  $-1$ ;
- $\mathcal{C}_+$  = region outside  $\mathcal{S}_{-+}$  ( $\mathcal{C}_+ = D \cap (\mathcal{C} \cup \mathcal{C}_-)^{\perp}$ ) where  $v = +1$ .

Changes on  $v$  occur only at crossing with the rules of Table 1.

### 4.2 Convergence for the nominal and perturbed system

For the nominal system we can assert the following:

change in $v$	switching surface	crossing direction
$+1 \rightarrow -1$	$\mathcal{S}_{+-}$	$\mathcal{C} \rightarrow \mathcal{C}_-$
$-1 \rightarrow +1$	$\mathcal{S}_{-+}$	$\mathcal{C} \rightarrow \mathcal{C}_+$

Table 1: Switching rules for  $v$ .

**Theorem 1** *Under the assumptions of invariance of  $\mathcal{E}$ , the system (4) with the two controllers (11) and (15) respectively for the cases  $v = -1$  and  $v = +1$  and with the feedback rule of Table 1 for  $v \in \mathcal{I}$ , asymptotically converges to the origin in backward motion from any initial condition in  $D$ .*

**Proof** From the analysis of Section 3 and looking at the switching rules of Table 1, the following order relation is the only possible one for the system:

$$\begin{array}{ccccc} \mathcal{C}_+ & \rightarrow & \mathcal{C} & \rightarrow & \mathcal{C}_- \\ v = +1 & & v = +1 & & v = -1 \end{array}$$

In fact, from any  $\mathbf{p}_0 \in D$ , the controller (15) steers the system inside  $\mathcal{S}_{+-}$  and  $\mathcal{S}_{-+}$  is a positively invariant set for the controller (11) ■

So for the nominal system the switching surface  $\mathcal{S}_{-+}$  is never in use. Due to the unstable equilibrium point, the effect of perturbations is critical in  $\mathcal{C}_-$ . Since the whole stabilization developed here occurs along a trajectory, we cannot expect the disturbances affecting the system to be vanishing at the equilibrium point of (12). When a perturbation is large enough to pull the state out of  $\mathcal{E}$  the system diverges. Trying to quantify the amplitude of the destabilizing perturbations and consequently trying to infer total stability for a class of bounded perturbations is very hard in our situation because of the input saturation involved. The destabilized system keeps driving backwards until it hits the  $\mathcal{S}_{-+}$  surface. After that, it inverts the direction of motion and try again to converge inside  $\mathcal{S}_{+-}$  with the forward controller.

As said above, if the  $\mathcal{S}_{-+}$  and  $\mathcal{S}_{+-}$  do not touch each other, then degenerate switching phenomena (normally referred to as Zeno chattering) do not occur. Furthermore, also the different pole placement philosophy adopted in the two controllers (11) and (15) (in one the critical mode, the  $\theta_3$  mode, is slow, in the other it is instead faster) is meant to avoid a chattering type of behavior (like keep moving the system back and forth between the same points on  $\mathcal{S}_{-+}$  and  $\mathcal{S}_{+-}$ ) which can happen if the two closed-loops resemble each other.

## 5 Experimental results

The controller for the truck and trailer shown in Figure 1 was implemented using a commercial version of PC/104 with an AMD586 processor and with an acquisition board for the sensor readings. For the relative angles  $\beta_2$  and  $\beta_3$  we used AD Converter provided with the acquisition board while the distance from the target line ( $y_3$ ) and the angle of the trailer with respect this line ( $\theta_3$ ) were measured using a Digital Input/Output Port. These inputs were read by a Interrupt Service Routine called at a frequency of 2kHz. This frequency and the 500 pulse shaft ensured a maximum speed of about 0.2 m/s which was sufficient for this application. The error on the relative angles is about 3-4 degrees due to a very high resistance of the potentiometers with respect the voltage applied (5V). To reduce it the values of the angles were averaged over 5 measures. The error on the angle of the trailer, due to the encoders, is given by the resolution of the encoder itself and it is less than 0.7 degrees while the error on the linear distance (along  $x_3$  and  $y_3$ ) is about 0.4 mm. The controller was written in C and used at a frequency of about 10Hz since the velocity of the system was very low.

Fig. 4-6 present the result of a simple real manouvre. The switching scheme used is the two-state automaton described in Section 4. The states and input are plotted versus the distance travelled. The manouvre is shown in Fig. 7 using the experimental data. The vehicle starts with saturated relative angles and first drives forward in order to realigne itself, then reverse along the reference line. The transient in  $y_3$  is very long and only a part of it is shown. Notice that since the  $\theta_3$  mode is slower than those of the relative angles most of the forward motion is needed to get  $\theta_3$  inside the ellipsoid  $\mathcal{S}_{+-}$ . Finally, in Figure 6 it is instructive to compare the activity of the feedback input when the open loop system is stable (upper plot) and when it is unstable (lower plot).

## References

- [1] C. Altafni. Controllability and singularities in the  $n$ -trailer system with kingpin hitching. Proc. 14th IFAC World Congress, vol. Q, p.139-145, Beijing, China.
- [2] P. Bolzern, R.M. De Santis, A. Locatelli and D. Masiocchi. Path-tracking for articulated vehicles with off-axle hitching. *IEEE Transaction on Control Systems Technology*, 6:515-523, 1998.
- [3] D.F. Hougen, M. Gini and J. Slagle. Rapid unsupervised connectionist learning for backing a robot with

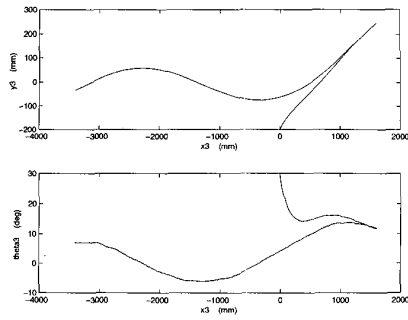


Figure 4:  $y_3$  displacement and  $\theta_3$  angle.

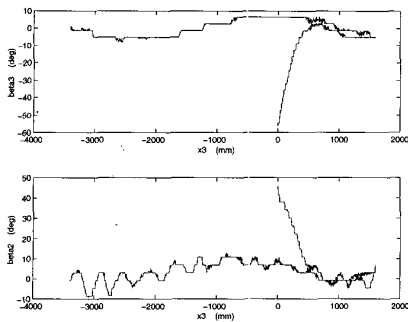


Figure 5: Relative angles  $\beta_3$  and  $\beta_2$ .

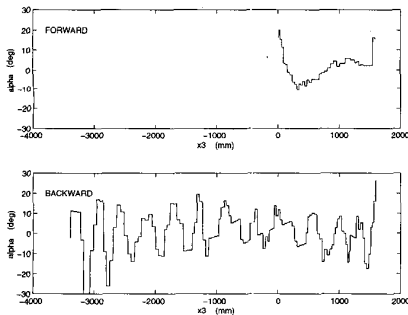


Figure 6: Steering input  $\alpha$  (forward and backward are plotted separately to avoid confusion as they consistently overlay).

two trailers. Proc. 1997 IEEE Int. Conf. on Robotics and Automation, p.2950-2955, Albuquerque, NM.

[4] D.H Kim and J.H Oh. Experiments of backward tracking control for trailer system. Proc. 1999 Int. Conf. on Robotics and Automation, p.19-22, Detroit, MI.

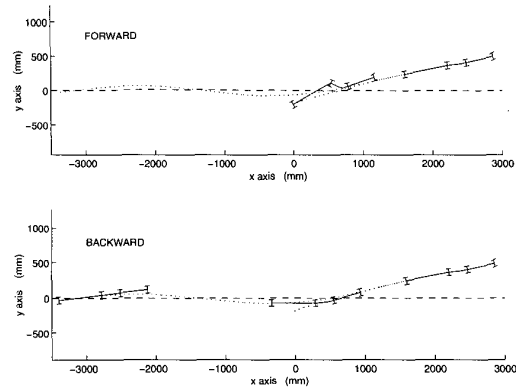


Figure 7: Sketch of the motion of the vehicle for the data of Fig. 4-6. The dotted line represents the path followed by the  $(x_3, y_3)$  point.

[5] G.S. Kong and B. Kosko. Adaptive fuzzy systems for backing up a truck and trailer. *IEEE Trans. on Neural Networks*, **3**:211-223, 1992.

[6] F. Lamiroux and J.P. Laumond. A practical approach to feedback control for a mobile robot with trailer. Proc. 1998 IEEE Int. Conf. on Robotics and Automation, p.3291-3296, Leuven Belgium.

[7] J.P. Laumond (ed). Robot Motion Planning and Control, Lecture notes in control and information sciences, Springer-Verlag, 1998.

[8] Y Nakamura, H. Ezaki, Y. Tan; W. Chung. Design of steering mechanism and control of nonholonomic trailer systems. Proc. 2000 IEEE Int. Conf. on Robotics and Automation, p.247 - 254, San Francisco, CA.

[9] D. Nguyen and B-Widrow. The truck backer-upper: an example of self-learning in neural networks. Proc. of SPIE vol.1293, pt.1,p.596-602, 1990.

[10] R. Parra-Loera and D.J. Corelis. Expert system controller for backing-up a truck-trailer system in a constrained space. Proc. of the 37th Midwest Symposium on Circuits and Systems p.1357-1361,1995.

[11] M. Sampei, T. Tamura, T. Kobayashi and N. Shibui. Arbitrary path tracking control of articulated vehicles using nonlinear control theory. *IEEE Transaction on Control Systems Technology*, **3**, 125-131, 1995.

[12] K. Tanaka, T. Taniguchi and H.O. Wang. Trajectory control of an articulated vehicle with triple trailers. Proc. 1999 IEEE International Conference on Control Applications, p.1673-8.